Acta Crystallographica Section E
Structure Reports Online
ISSN 1600-5368

$YbMn_6Sn_6$

Sheng-Qing Xia and Svilen Bobev*

Department of Chemistry and Biochemistry, University of Delaware, Newark, DE 19716, USA

Correspondence e-mail: sbobev@chem.udel.edu

Key indicators

Single-crystal X-ray study
T = 120 K
Mean σ(Sn–Mn) = 0.004 Å
Disorder in main residue
R factor = 0.041
wR factor = 0.091
Data-to-parameter ratio = 9.0

For details of how these key indicators were automatically derived from the article, see http://journals.iucr.org/e.

Received 18 November 2005
Accepted 1 December 2005
Online 7 December 2005

Single crystals of the title compound, ytterbium hexamanganese hexastannide, were serendipitously synthesized from a reaction of elemental Yb, Mn and Bi in an Sn flux. The structure was determined by single-crystal X-ray diffraction to be an intermediate ordered state of the $HfFe_6Ge_6$ and YCo_6Ge_6 structures. This result confirms previous work on the structure of $YbMn_6Sn_6$ from X-ray and neutron powder diffraction data [Mazet *et al.* (1999). *J. Magn. Magn. Mater.* **204**, 11–19], although the statistical distribution of Yb and Sn on the partially occupied sites is determined to be significantly different.

Comment

In the past decade, there have been several reports of intermetallic phases that exhibit very large magnetoresistance in moderate magnetic fields. Among these, Mn-containing zintl compounds from the $E_{14}MnPn_{11}$ family (E is alkaline earth or divalent rare earth metals, and Pn are pnicogens, *i.e.* P, As, Sb or Bi) are the most frequently reccurring ones, and their crystal chemistry and physical properties have been extensively studied (Young *et al.*, 1995; Webb *et al.*, 1998). These discoveries have motivated many further studies and, to date, several new polar intermetallics, *i.e.* formed between metals with largely different electronegativities, have been reported (Holm *et al.*, 2003; Kim *et al.*, 2000; Nirmala *et al.*, 2005). All these new compounds feature condensed $MnPn_4$ building blocks and exhibit unusual physical properties due to direct or indirect Mn···Mn interactions.

Intrigued by the rich phenomenology of these Mn-containing phases, we have undertaken systematic studies of the corresponding E–Mn–Bi systems, aimed primarily at synthesizing $E_9Mn_{4+x}Bi_9$, isostructural with the recently revised $Ca_9Zn_{4+x}Sb_9$ (x = 0.5) (Bobev *et al.*, 2004), and examination of their physical properties. It was anticipated that, by employing metals with low melting points, such as Sn for instance, the target materials could be synthesized as large crystals and in high yield. However, Sn flux reactions in the system Yb–Mn–Bi have been found to produce small crystals of the desired $Yb_9Mn_{4+x}Bi_9$ phase in very low yield. Quantitative product formations from such reactions are the body-centred tetragonal $Yb_{11}Bi_{10}$, with the $Ho_{11}Ge_{10}$ type structure (Smith *et al.*, 1967), and the title compound, $YbMn_6Sn_6$. The latter is shown to be a room-temperature ferromagnet with strong coupling between the Mn spins, and its structure has been previously studied by means of powder diffraction (Mazet *et al.*, 1999). This study also suggested that the hexagonal $YbMn_6Sn_6$ structure (Figs. 1 and 2) exhibits features pertinent to both the $HfFe_6Ge_6$ (Olenitch *et al.*, 1981) and the YCo_6Ge_6-types (Malaman *et al.*, 1997). Both types are closely

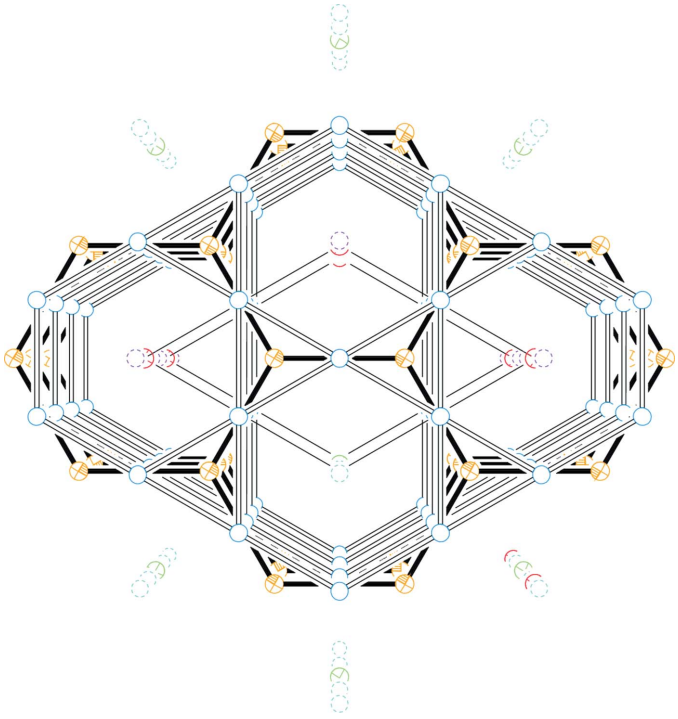

Figure 1
A perspective view of the crystal structure of $YbMn_6Sn_6$, down the [001] direction, with the unit cell outlined. Displacement ellipsoids are drawn at the 92% probability level. Atoms Sn1 and Sn2 are shown with full yellow ellipsoids, Mn atoms are drawn as blue outline ellipsoids, and the partially occupied atoms Sn3*A* and Sn3*B* are shown as purple and light-blue dotted outline ellipsoids, respectively. Atoms Yb1*A* and Yb1*B* are represented by red and green crossed ellipsoids, respectively. Some of the 50% occupied positions have been left empty to exemplify the disorder.

related to the common $CaCu_5$ structure (Buschow & Van der Goot, 1971).

Using this formalism, the $YbMn_6Sn_6$ structure can be viewed as a stacking of ordered graphite-like layers of Sn atoms (Sn1 at $z = \frac{1}{2}$ and Sn2 at $z = 0$), and ordered Kagome-type layers of Mn atoms [Mn at Wyckoff position 6*i* at $(\frac{1}{2}, 0, \frac{1}{4})$], as shown in Fig. 2. Between these ordered hexagonal layers are the disordered Sn3*A* and Sn3*B* sheets. The Yb atoms also form layers perpendicular to the *c* axis at $z = 0$ (Yb1*A*) and $z = \frac{1}{2}$ (Yb1*B*), *i.e.* within the Sn2 and Sn1 layers, respectively.

The distances (Table 1) between the fully occupied positions, as well as the anisotropic displacement parameters for all atoms, are very reasonable. However, the contacts between the partially occupied atoms Yb1*A* and Sn3*B*, and Yb1*B* and Sn3*A*, respectively, are unrealistic (*ca* 1.5 Å). This means that whenever Yb1*A* or Yb1*B* are present, Sn3*B* and Sn3*A* are missing and *vice versa*. This model implies that a superstructure with a doubled *c* axis could exist, but long-exposure images failed to provide evidence for such a supercell. Indication for this structural disorder has also been found in the X-ray powder diffraction patterns of $YbMn_6Sn_6$ (Mazet *et al.*, 1999). The presence of weaker *hkl* ($l = 2n + 1$) Bragg reflections than those observed in $MgMn_6Sn_6$ has been interpreted as a result of statistically disordered sites, as in the related $SmMn_6Sn_6$ (Malaman *et al.*, 1997). Rietveld refinements of

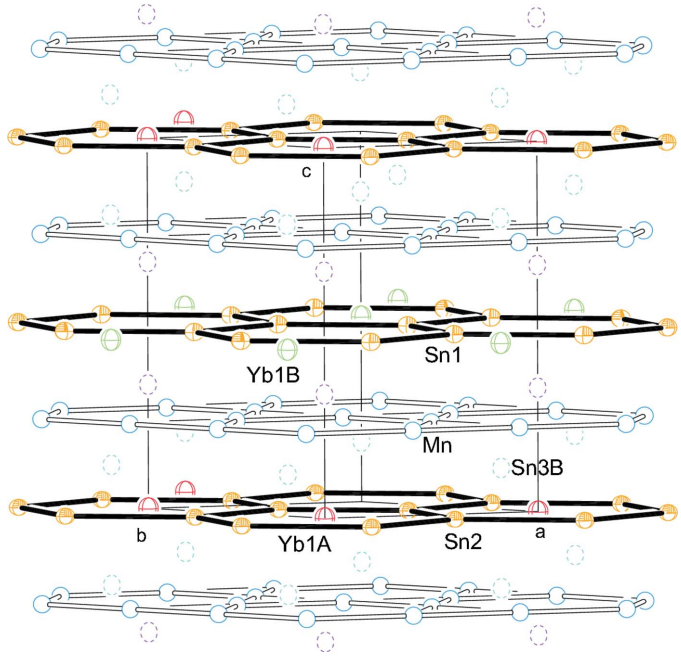

Figure 2
A perspective view of the crystal structure of $YbMn_6Sn_6$, approximately down the [110] direction. Colour code as in Fig. 1.

these powder data (Mazet *et al.*, 1999) support this model, with atomic arrangements giving a mixed distribution of 77 (1):23 (1) and 23 (1):77 (1) on four different sites, Yb1*A*/Yb1*B* and Sn3*A*/Sn3*B*, respectively. The results from our single-crystal diffraction work show a different distribution of 52 (2):48 (2) and 56 (1):44 (1) for the two pairs of sites, respectively. This difference in the refinements is most likely due to the different synthetic routes, *i.e.* flux growth in the present case *versus* arc melting and annealing in the previous work. Examples of various ordering transitions depending on the annealing temperatures are known already for some other EMn_6Sn_6 compounds (*E* = Mg, Sc, Y, Zr, Pr, Sm, Nd, Gd–Tm) (Mazet *et al.*, 1999).

Experimental

All manipulations were carried out under argon or *in vacuo*. For the synthesis, pure elements were used as received: Yb (Ames Laboratory, ingot, 99.99% metal basis), Mn (Alfa, pieces, 99.98%), Bi (Alfa, shot, 99.99%) and Sn (Alfa, shot, 99.99%). The reagents were loaded into an alumina crucible in the ratio Yb:Mn:Bi:Sn = 9:6:9:29, and were subsequently sealed in an evacuated fused silica ampoule. The following heating profile was employed for the reaction: heating from room temperature to 1223 K at a rate of 25 K h^{-1}, dwell at 1223 K for 10 h, then cooling to 1073 K at a rate of 5 K h^{-1}. At this temperature, the mixture was allowed to dwell again for 72 h. After cooling to 873 K over a period of 10 h, the excess flux was removed by centrifugation. The products of the reaction consist of two kinds of crystals, namely $Yb_{11}Bi_{10}$ (main product, dark-to-black crystals of irregular shape) and hexagonal $YbMn_6Sn_6$ (minor product, silver needle-like crystals).

Crystal data

$YbMn_6Sn_6$	Mo $K\alpha$ radiation
M_r = 1214.82	Cell parameters from 1336 reflections
Hexagonal, $P6/mmm$	θ = 2.3–27.0°
a = 5.5117 (13) Å	μ = 32.93 mm^{-1}
c = 8.989 (4) Å	T = 120 (2) K
V = 236.49 (14) Å^3	Block cut from needle, grey
Z = 1	0.06 × 0.05 × 0.04 mm
D_x = 8.530 Mg m^{-3}	

Data collection

Bruker SMART APEX diffractometer	144 independent reflections
ω scans	99 reflections with $I > 2\sigma(I)$
Absorption correction: multi-scan (*SADABS*; Sheldrick, 2003)	R_{int} = 0.023
T_{min} = 0.142, T_{max} = 0.268	θ_{max} = 27.0°
1336 measured reflections	$h = -6 \rightarrow 7$
	$k = -7 \rightarrow 7$
	$l = -11 \rightarrow 11$

Refinement

Refinement on F^2	$(\Delta/\sigma)_{max}$ = 0.010
$R[F^2 > 2\sigma(F^2)]$ = 0.041	$\Delta\rho_{max}$ = 1.18 e Å^{-3}
$wR(F^2)$ = 0.091	$\Delta\rho_{min}$ = −1.49 e Å^{-3}
S = 1.51	Extinction correction: *SHELXTL* (Sheldrick, 2001)
144 reflections	Extinction coefficient: 0.021 (3)
16 parameters	
$w = 1/[\sigma^2(F_o^2) + 22.0394P]$ where $P = (F_o^2 + 2F_c^2)/3$	

Table 1
Selected bond lengths (Å).

Yb1*A*—Sn3*A*	3.013 (7)	Sn1—Mn1^{i}	2.760 (4)
Yb1*A*—Sn2	3.1822 (7)	Sn2—Mn1^{i}	2.747 (4)
Yb1*B*—Sn3*B*	3.022 (7)	Mn1—Sn3*B*	2.861 (2)
Yb1*B*—Sn1	3.1822 (7)	Mn1—Sn3*A*	2.862 (2)

Symmetry code: (i) $-y, x-y, z$.

In the structure refinement, the full occupancies for all sites were verified by freeing the site occupation factor for an individual atom, while the remaining parameters were kept fixed. This proved that the Sn1, Sn2 and Mn positions are fully occupied with corresponding deviations from full occupancy within 3σ. Site occupation factors for Yb1*A* and Yb1*B*, and for Sn3*A* and Sn3*B*, refined close to 50% and were finally modelled as a 50:50 statistical mixture. The maximum peak and deepest hole are located 0.11 Å from Sn3*B* and coincident with Yb1*B*, respectively.

Data collection: *SMART* (Bruker, 2002); cell refinement: *SAINT* (Bruker, 2002); data reduction: *SAINT*; program(s) used to solve structure: *SHELXTL* (Sheldrick, 2001); program(s) used to refine structure: *SHELXTL* (Sheldrick, 2001); molecular graphics: *XP* in *SHELXTL*; software used to prepare material for publication: *SHELXTL*.

This work was funded in part by a University of Delaware start-up grant.

References

Bobev, S., Thompson, J. D., Sarrao, J. L., Olmstead, M. M., Hope, H. & Kauzlarich, S. M. (2004). *Inorg. Chem.* **43**, 5044–5052.

Bruker (2002). *SMART* and *SAINT*. Bruker AXS Inc., Madison, Wisconsin, USA.

Buschow, K. H. J. & van der Goot, A. S. (1971). *Acta Cryst.* B**27**, 1085–1088.

Holm, A. P., Olmstead, M. M. & Kauzlarich, S. M. (2003). *Inorg. Chem.* **42**, 1973–1981.

Kim, H., Condron, C. L., Holm, A. P. & Kauzlarich, S. M. (2000). *J. Am. Chem. Soc.* **122**, 10720–10721.

Malaman, B., Venturini, G., Chafik EI Idrissi, B. & Ressouche, E. (1997). *J. Alloys Compnd* **252**, 41–49.

Mazet, T., Welter, R. & Malaman, B. (1999). *J. Magn. Magn. Mater.* **204**, 11–19.

Nirmala, R., Morozkin, A. V., Suresh, K. G., Kim, H.-D., Kim, J.-Y., Park, B.-G., Oh, S.-J. & Malik, S. K. (2005). *J. Appl. Phys.* **97**, 10M511–3.

Olenitch, R. R., Aksel'rud, L. G. & Yarmolyuk, Ya. P. (1981). *Dopov. Akad. Nauk Ukrain. RSR Ser. A*, **43**, 87–91. (In Ukrainian).

Sheldrick, G. M. (2001). *SHELXTL*. Bruker AXS Inc., Madison, Wisconsin, USA.

Sheldrick, G. M. (2003). *SADABS*. University of Göttingen, Germany.

Smith, G. S., Johnson, Q. & Tharp, A. G. (1967). *Acta Cryst.* **23**, 640–644.

Webb, D. J., Cohen, R., Klavins, P., Shelton, R. N., Chan, J. Y. & Kauzlarich, S. M. (1998). *J. Appl. Phys.* **83**, 7192–7194.

Young, D. M., Torardi, C. C., Olmstead, M. M. & Kauzlarich, S. M. (1995). *Chem. Mater.* **7**, 93–101.